

# Design Proposal: Compact Modeling and Linearized FSR Analysis for SOI MZI Design

Sheng-Xun Su, edX Username: sususteven5245@gmail.com  
Course: UBCx Phot1x - Silicon Photonics Design, Fabrication and Data Analysis  
New Taipei City, Taiwan

**Abstract**—This report describes the design of Mach-Zehnder interferometers (MZIs) on a silicon-on-insulator platform using strip waveguides. Waveguide-level simulations and analytical evaluations are performed to support the proposed design choices. Multiple MZI devices with different path length differences are designed to examine the dependence of the free spectral range (FSR) on the interferometer imbalance. A linearized analysis based on the reciprocal path length difference is explored to relate the simulated FSR to the waveguide group index. A first-draft layout is also presented for future fabrication and automated testing.

**Index Terms**—Silicon Photonics, Silicon-on-Insulator (SOI), Mach-Zehnder Interferometer (MZI), Passive Components.

## I. INTRODUCTION

The Mach-Zehnder Interferometer (MZI) is a fundamental component in silicon photonics, finding extensive applications in optical modulators, optical switches, and sensors. This research focuses on establishing a comprehensive MZI design workflow, spanning from waveguide modeling to circuit-level simulation. Furthermore, a linearized Free Spectral Range (FSR) analysis method is introduced to provide an additional consistency check for the extracted group index at this proposal stage.

## II. THEORY

### A. MZI Transfer Function

Consider an unbalanced Mach-Zehnder Interferometer (MZI) where the input light is split into two arms by a Y-branch. After propagating through waveguides of lengths  $L_1$  and  $L_2$ , the light is recombined. The transfer function  $T_{MZI}(\lambda)$  can be expressed as [1]:

$$T_{MZI}(\lambda) = \frac{1}{2}[1 + \cos(\beta\Delta L)] \quad (1)$$

where  $\beta = 2\pi n_{eff}/\lambda$  is the propagation constant and  $\Delta L = L_2 - L_1$  represents the path length difference. This expression assumes ideal 50:50 power splitting and negligible imbalance or excess loss, which is sufficient for FSR analysis.

### B. Free Spectral Range (FSR)

The Free Spectral Range (FSR) is defined as the wavelength spacing between two adjacent transmission peaks:

$$FSR = \frac{\lambda^2}{n_g \Delta L} \quad (2)$$

where  $n_g$  is the group index, defined as  $n_g = n_{eff} - \lambda \frac{dn_{eff}}{d\lambda}$ .

### C. Linear Relationship between FSR and $1/\Delta L$

In this work,  $\lambda$  is set to 1550 nm for simplicity, where the compact model is defined, and the dispersion within the considered bandwidth is sufficiently small. By rewriting the FSR equation, we obtain a linear relationship:

$$FSR = \left( \frac{\lambda^2}{n_g} \right) \cdot \left( \frac{1}{\Delta L} \right) \quad (3)$$

This representation linearizes the relationship between FSR and the reciprocal of the path length difference ( $1/\Delta L$ ), where the slope is  $\lambda^2/n_g$ . This approach is advantageous for:

- **Data Visualization:** Linear plots are more intuitive than hyperbolic ones.
- **Parameter Extraction:** The group index  $n_g$  can be estimated through linear fitting.
- **Model Accuracy:** The linear fitting provides a quantitative measure of internal consistency between the model and simulation results.

## III. WAVEGUIDE MODELING

### A. Simulation Settings

A strip waveguide with cross-sectional dimensions of 500 nm × 220 nm was analyzed using the Lumerical MODE Finite Difference Eigenmode (FDE) solver. The simulation parameters were configured as follows:

- **FDE Region:** 5.0 μm (X-span) × 1.7 μm (Y-span).
- **Mesh Grid:** 100 × 100.
- **Boundary Conditions:** Metal boundaries.
- **Materials:** Si (Palik) and SiO<sub>2</sub> (Palik) using Palik material data with multi-coefficient fitting over the wavelength range of (1.2 to 1.8 μm), the fitting tolerances are set to 0.1 and 0.001.

### B. Modal Characteristics

The modal properties at the operating wavelength of 1550 nm are summarized in Table I. The fundamental TE mode field distribution is shown in Fig. 1.

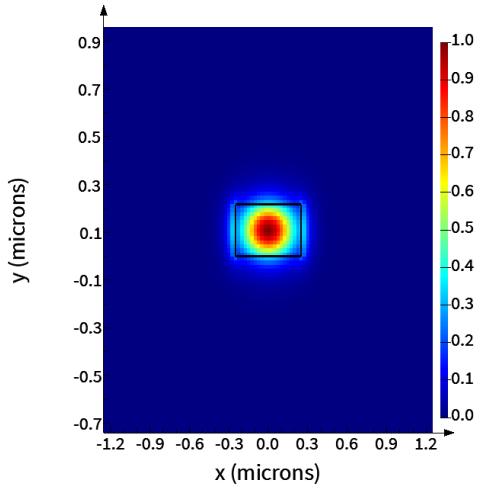


Fig. 1. Electric field intensity distribution of the fundamental TE mode at 1550 nm.

TABLE I  
SIMULATED WAVEGUIDE MODAL PARAMETERS AT A WAVELENGTH OF  
1550 NM.

Parameter	Value
$n_{eff}$	2.5034
$n_g$	4.1967
Loss (dB/cm)	$4.72 \times 10^{-4}$
TE purity	99%

### C. Dispersion Characteristics

Wavelength sweeping from 1500 nm to 1600 nm revealed the following trends. The wavelength-dependent behaviors of  $n_{eff}$  and  $n_g$  are illustrated in Fig. 2 and Fig. 3, respectively.

- $n_{eff}$  decreases with increasing wavelength, exhibiting normal dispersion.
- $n_g$  increases slightly with wavelength (approximately 4.197 to 4.210).

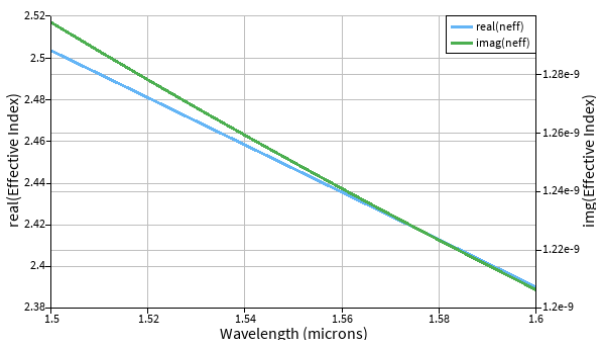


Fig. 2. Simulated effective index ( $n_{eff}$ ) of the SOI strip waveguide as a function of wavelength.

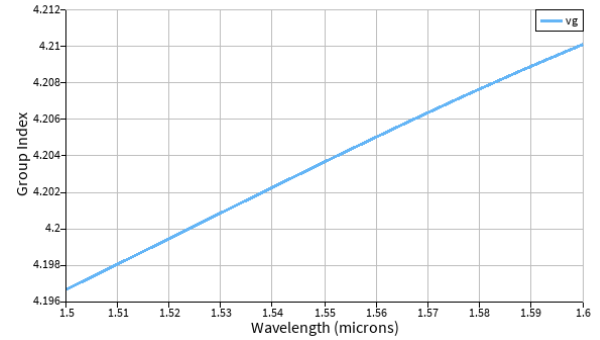


Fig. 3. Simulated group index ( $n_g$ ) of the SOI waveguide as a function of wavelength.

### D. Compact Model

To facilitate circuit-level simulation, a second-order Taylor expansion was used to establish a compact model for  $n_{eff}$  at a center wavelength of 1.55  $\mu$ m. This model was implemented using a Lumerical MODE script which is

$$n_{eff}(\lambda) = 2.4468 - 1.1334(\lambda - 1.55) - 0.04394(\lambda - 1.55)^2 \quad (4)$$

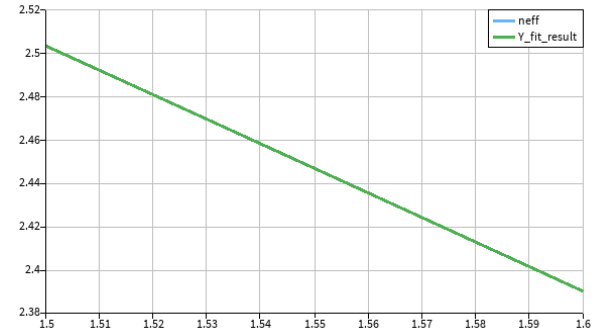


Fig. 4. Second-order Taylor expansion compact model of the SOI waveguide effective index extracted from MODE simulations.

## IV. MZI DESIGN AND SIMULATION

### A. Circuit Implementation

The MZI circuit was implemented in Lumerical INTERCONNECT [2] using the compact model derived above for the waveguides. For the input/output coupling and power splitting, standard passive components from the SiEPIC EBeam PDK [3] were utilized:

- **Grating Couplers (GCs):** Standard TE-mode focusing grating couplers were used to couple light between the optical fiber and the chip.
- **Y-Branche:** Optimized adiabatic Y-branch splitters were used to ensure 50:50 power splitting with minimal insertion loss.
- **Optical Network Analyzer (ONA):** Used for frequency domain characterization within the simulation environment.

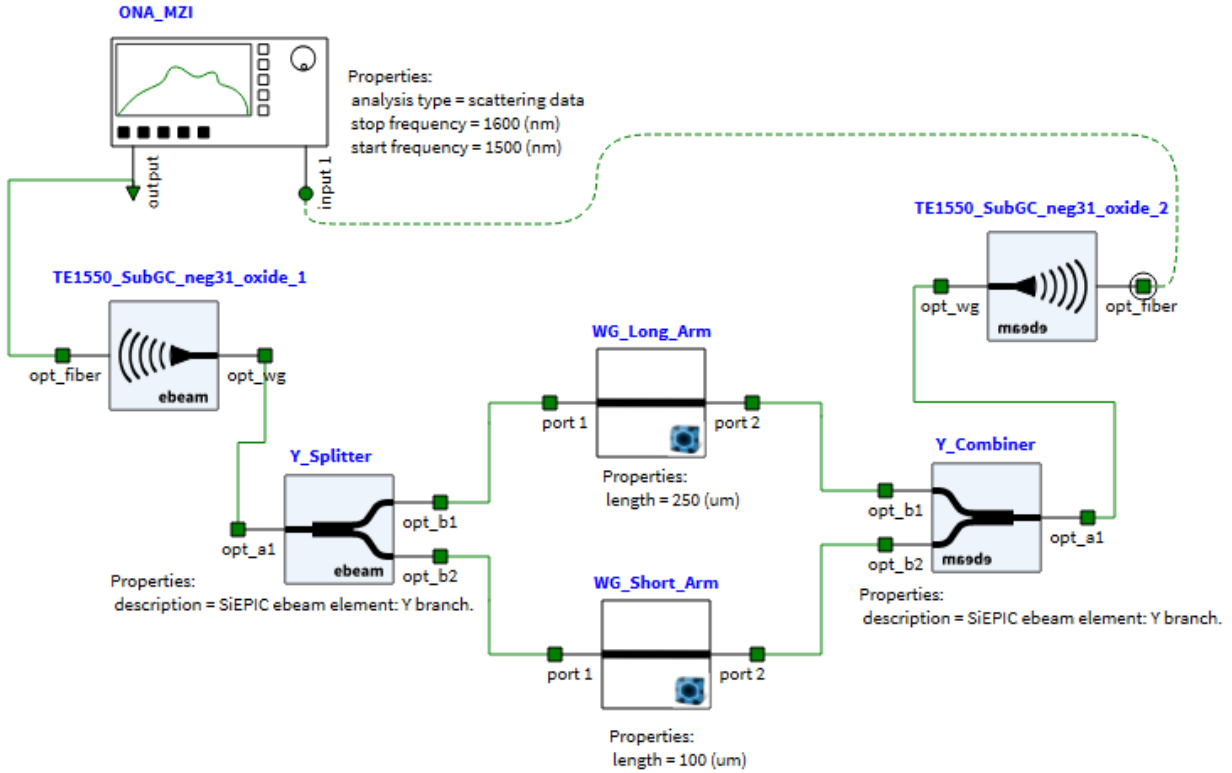


Fig. 5. MZI circuit schematic implemented in INTERCONNECT. The configuration shown corresponds to  $\Delta L = 150 \mu\text{m}$  (long arm:  $250 \mu\text{m}$ , short arm:  $100 \mu\text{m}$ ) as a representative example. Other MZI variants were simulated by adjusting the arm lengths accordingly.

### B. Design Specifications and Results

Table II summarizes the design parameters for five MZI configurations with different path length differences ( $\Delta L$ ) and compares the theoretical FSR with simulation results.

TABLE II

MZI DESIGN PARAMETERS AND SIMULATION RESULTS. THEORETICAL VALUES WERE CALCULATED USING EQ. (2), WHILE SIMULATED VALUES WERE OBTAINED FROM INTERCONNECT.

$\Delta L (\mu\text{m})$	Theoretical FSR (nm)	Simulated FSR (nm)	Error (%)
50	11.44	11.32	-1.1
100	5.72	5.68	-0.7
150	3.81	3.79	-0.5
200	2.86	2.83	-0.9
250	2.29	2.28	-0.6

### C. FSR Characteristics and Group Index Verification

To further verify the consistency of the MZI model, the relationship between the free spectral range (FSR) and the inverse path length difference ( $1/\Delta L$ ) was linearized. A linear regression was performed on the five simulated data points listed in Table II using MATLAB, yielding the following results:

- Coefficient of Determination ( $R^2$ ): 0.999996
- Extracted Group Index ( $n_g$ ): 4.247

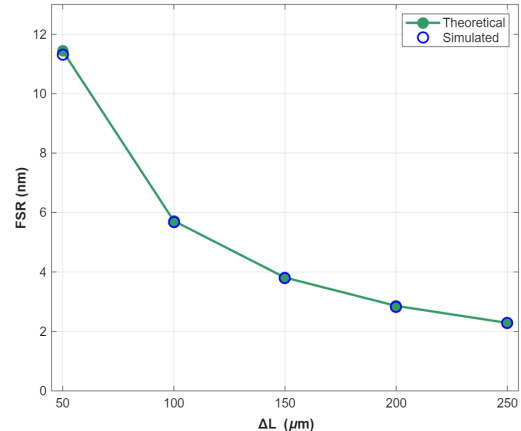


Fig. 6. Linearized free spectral range (FSR) as a function of  $1/\Delta L$  obtained from the five simulated MZI devices listed in Table II.

To further validate the extracted group index, the results obtained from two independent methods are compared below:

- **Method 1 (MODE Direct Calculation):**  $n_g = 4.1967$
- **Method 2 (FSR Linear Fitting):**  $n_g = 4.247$
- **Relative Difference:** 1.23%

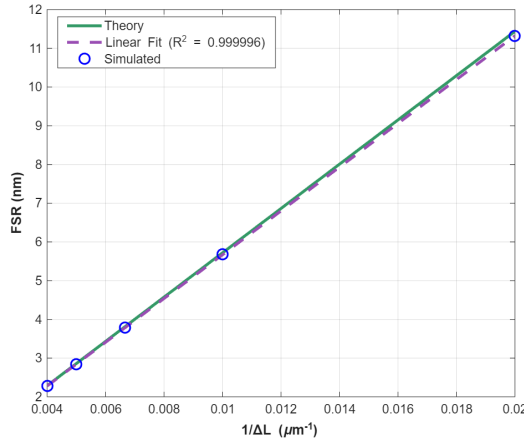


Fig. 7. Linear regression analysis of the FSR versus  $1/\Delta L$  relationship using the five simulated MZI devices.

The small difference of 1.23% shows that the independent analysis methods are consistent. This confirms that the compact model derived from MODE software correctly represents the MZI behavior in INTERCONNECT software.

#### D. Transmission Characteristics and Loss Analysis

The transmission spectra for the  $\Delta L = 150 \mu\text{m}$  configuration were analyzed (Fig. 8). Key observations include:

- **Ideal MZI (without Grating Couplers):** Peak transmission  $\approx 0 \text{ dB}$ , with an extinction ratio (ER) exceeding 60 dB.
- **MZI with Grating Couplers (GCs):** Peak transmission  $\approx -6 \text{ dB}$ , primarily due to the insertion loss of two GCs.
- **Loss Breakdown:** The total loss is dominated by the GCs ( $\sim 6 \text{ dB}$  total), while the Y-branch splitters and waveguide propagation are significantly lower and have a minimal impact on the overall transmission level.

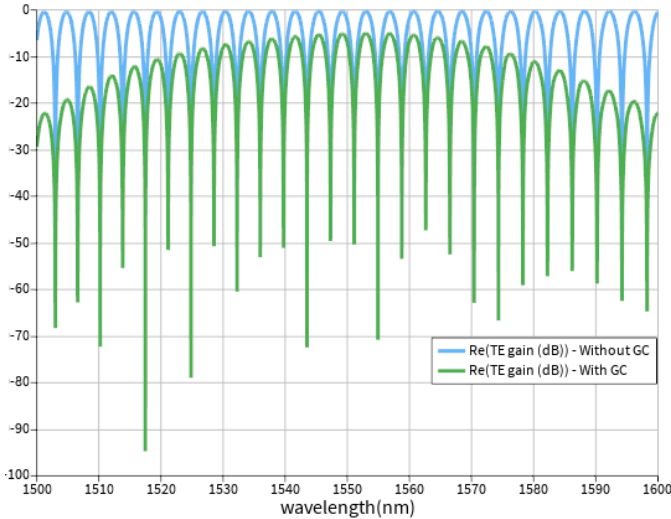


Fig. 8. Simulated transmission spectrum of the MZI with  $\Delta L = 150 \mu\text{m}$ .

#### V. LAYOUT DESIGN

The physical layout was designed for fabrication with a total footprint of  $410 \mu\text{m} \times 605 \mu\text{m}$ . The design features include:

- **Device Array:** Integration of five MZI devices with path length differences ( $\Delta L$ ) ranging from  $50 \mu\text{m}$  to  $250 \mu\text{m}$ .
- **Grating Coupler Pitch:** Pitch of  $127 \mu\text{m}$  was implemented to ensure compatibility with fiber arrays.
- **Bending Radius:** The waveguide bends required a radius sufficiently large to maintain consistency with the straight-waveguide compact model used in our circuit simulations.
- **Testing Orientation:** All grating couplers are oriented to the right to facilitate automated testing and alignment.

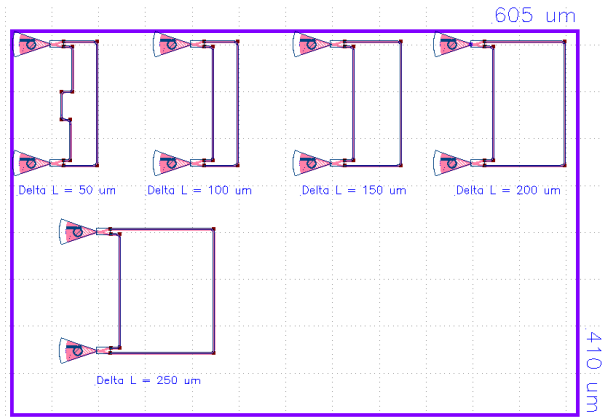


Fig. 9. Draft layout design for MZI devices with  $\Delta L$  ranging from 50 to  $250 \mu\text{m}$ .

#### VI. PRELIMINARY RESULTS AND DISCUSSION

The proposed design flow yielded the following significant results:

- 1) **Compact Model:** The second-order Taylor expansion achieved an excellent fit for the effective index ( $n_{eff}$ ) across the 1500 to 1600 nm wavelength range.
- 2) **FSR Linearization:** The  $FSR$  vs.  $1/\Delta L$  analysis exhibited a highly precise linear trend across the five simulated MZI designs, achieving a coefficient of determination ( $R^2$ ) of 0.999996.
- 3) **Dual Verification of  $n_g$ :** A low relative error of 1.23% was achieved between the two independent extraction methods.
- 4) **MZI Design Evaluation:** Five MZI variants were examined, showing theoretical-to-simulation FSR differences within 3%.

#### VII. RESULTS AND DISCUSSION

This section will combine the section of preliminary results and discussion in Final Report.

#### VIII. CONCLUSION

This section will be provided in the Final Report.

## REFERENCES

- [1] L. Chrostowski and M. Hochberg, *Silicon Photonics Design: From Devices to Systems*. Cambridge, UK: Cambridge University Press, 2015.
- [2] Lumerical Inc., “Ansys Lumerical MODE and INTERCONNECT Software,” [Online]. Available: <https://www.ansys.com/products/optics> (Accessed: Jan. 26, 2026).
- [3] L. Chrostowski, “The free spectral range (FSR) of the imbalanced interferometer,” *Lecture notes, edX UBCx: PhotIx*, 2015. [Online]. Available: <https://learning.edx.org/> (Accessed: Jan. 25, 2026).